

## Electrochemical Characteristics of Water-Soluble Phosphate-Functionalized Naphthalene- and Perylene-Bisimides and Their Zirconium Bisphosphate Multilayers on ITO Electrode

Kwang Je Cho, Yeong Il Kim\*, and Hyun Kwan Shim\*

Department of Chemistry, Pukyong National University, 45 Yongso-ro, Nam-gu, Busan 48513, Korea.

\*E-mail: [hkshim@pknu.ac.kr](mailto:hkshim@pknu.ac.kr)

(Received November 12, 2018; Accepted December 9, 2018)

**ABSTRACT.** N,N'-bis(ethylhydrogen phosphate)-1,4,5,8-naphthalene bis(dicarboximide) (EPNI) and N,N'-bis(ethylhydrogen phosphate)-3,4,9,10-perylene bis(dicarboximide) (EPPI) and their zirconium bisphosphate multilayers (Zr-EPNI and Zr-EPPI), that had been briefly reported by us, were further investigated in terms of their electrochemical properties. EPNI in aqueous solution showed typical two reversible reductions at ITO electrode but the reductions were strongly dependent on solution pH while EPPI showed only an irreversible reduction. The single and mixed multilayers of Zr-EPNI and Zr-EPPI were well constructed on ITO electrode by the alternate adsorptions of zirconium ion and the bisimides. While Zr-EPNI multilayer on ITO electrode showed single broad reversible reduction with  $E_{1/2} = -0.68$  V, Zr-EPPI gave two separated reductions at  $E_{1/2} = -0.54$  and  $-0.81$  V vs SCE, quite differently from the solution properties. The average layer densities of the multilayers were estimated as  $1.5 \times 10^{-10}$  and  $2.3 \times 10^{-10}$  mol/cm<sup>2</sup> for Zr-EPNI and Zr-EPPI, respectively. Both the monolayers of Zr-EPNI and Zr-EPPI could not completely block the electron transfer between  $\text{Fe}(\text{CN})_6^{3-}$  in solution and ITO electrode but 3–5 layers of Zr-EPNI and Zr-EPPI could block it completely and mediated the one-way electron transfer at the potential shifted to their reduction potentials. When the monolayer of zirconium 1,10-decanediylbisphosphonate (Zr-DBP) was used as a sublayer of Zr-EPNI and Zr-EPPI layers, the mediated electron transfer became prominent without any direct electron transfer.

**Keywords:** Perylene bisimide, Naphthalene bisimide, Zirconium bisphosphate multilayer

### INTRODUCTION

Naphthalene and perylene bisimides<sup>1</sup> have attracted much attention due to their photochemical and electrochemical properties such as high electron affinity and mobility, redox reversibility, high yield of fluorescence and high thermal stability as materials for solar cells, organic thin film transistor, electroluminescent devices and various organic electronic devices.<sup>2,3</sup> The thin film formation of these materials is essential for the application to electronic devices. The control of film thickness and orientation is also important factors. The Langmuir-Blodgett (LB) method has been known for a long time as one of the techniques of controlling thin films in molecular level and many efforts had been devoted to applying this technique to electronic devices. But LB method has not been so successful because of several constraints such that molecule must be amphiphilic, only planar substrate can be applicable, many repeated mechanical manipulations are required, and the formed film has low thermal stability. Metal bisphosphate/phosphonate multilayer technique has been known to provide a mean overcoming the several drawbacks of LB method because of a self-assembling hybridity between organic and inorganic

compounds.<sup>4</sup> Since this technique was introduced,<sup>5</sup> several functionalized metal bisphosphonate multilayers that might be used as a part of molecular electronic devices had been demonstrated for a while.<sup>6</sup> We once briefly reported the zirconium bisphosphate/phosphonate multilayers of naphthalene and perylene bisimides.<sup>7</sup> Politi and Brochsztain et al. also reported the zirconium bisphosphonate multilayers of these bisimides at a very similar time or later although the molecular structures were slightly different.<sup>8</sup> As mentioned before, naphthalene and perylene bisimides thin films can be very useful parts of molecular electronic devices because of their well-defined redox property. Since our and Politi et al.'s reports where the systematic multilayer constructions of the bisimides were mainly demonstrated, no other studies of these multilayers have been reported yet as far as we know. Therefore, we investigated these multilayers further in terms of their electrochemical properties. Here we studied first the properties of bis(ethyl phosphate)-linked naphthalene and perylene bisimides in solution and their zirconium bisphosphate multilayers on ITO electrode were electrochemically studied with another redox couple in solution.

## EXPERIMENTAL

### Materials

1,4,5,8-naphthalenetetracarboxylic dianhydride (NTCD, >95%), 3,4,9,10-perylenetetracarboxylic dianhydride (PTCD, 97%), 2-aminoethyl dihydrogen phosphate (98%), zirconyl chloride octahydrate (98%), triethyl phosphite (98%), phosphoryl chloride (99%), 1,6-lutidine (>99%), 1,10-dibromodecane (97%) and potassium ferricyanide (99%) were all purchased from Sigma-Aldrich. Imidazole was obtained from Alfa-Aesar. Indium-tin-oxide (ITO) glass ( $< 20 \Omega/\square$ ) were obtained from Samsung-Corning. All other chemicals were reagent grade and used as received. Water was purified to  $> 18.0 \text{ M}\Omega\text{cm}$  resistivity by Barnstead Nanopure II water purification system.

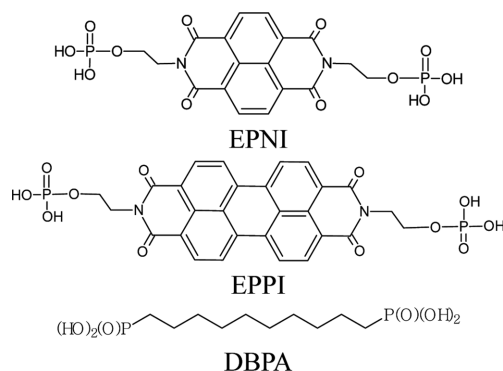
### Apparatus

UV-Vis absorption spectra were measured with Varian Cary 1 and Ocean Optics Maya 2000 spectrometers. EG&G 263A and Gamry PCI4/750 potentiostats were employed for cyclic voltammetric measurements in a standard three-electrode cell. IR spectra were observed with Perkin-Elmer spectrum 2000 spectrometer.

### Preparation

EPNI and EPPI were synthesized by the condensation reactions of NTCD and PTCD, respectively with 2-aminoethyl dihydrogen phosphate in molten imidazole as previously reported.<sup>7b</sup> For EPPI specifically, 1.00 g of PTCD and 1.10 g of 2-aminoethyl dihydrogen phosphate were heated in 20.0 g of molten imidazole to 140 °C and remained for about 20 min. The color of the reaction mixture was abruptly changed from red to dark red during the reaction. After the color change the heating was stopped and the reaction mixture was cooled to room temperature. Acetone was poured to the mixture in order to remove imidazole and the reactants. The product was filtered and washed with acetone several times. The filtered product was dissolved in water and acidified with HCl to reprecipitate the product as acid form. The product was confirmed with IR data ( $1692$  and  $1644 \text{ cm}^{-1}$  of imide CO peaks) and elemental analysis data (C: 53.11, H: 3.35, N: 4.47, O: 29.3%). EPNI was also prepared in the same way except the temperature and reaction time. The reaction was done at 170 °C for 1 h. EPNI was very hygroscopic and could not be precipitated as acid form. After acidification the product was isolated by the evaporation of water and excess HCl. EPNI was also confirmed with IR data ( $1707$  and  $1673 \text{ cm}^{-1}$  of imide CO peaks). 1,10-decanediyl bis(phosphonic acid) (DBPA) was

prepared by the Michaelis-Arbuzov reaction of 1,10-bromodecane and triethyl phosphite as previously reported.<sup>9</sup>



The multilayers of Zr-EPNI and Zr-EPPI on the planar substrates of glass, quartz and ITO/glass were prepared by the alternate dipping between 0.5 mM EPNI or EPPI solution and 20 mM  $\text{ZrOCl}_2$  solution at room temperature. Each dipping was kept for ca. 10 min and the thorough washing was done with a copious amount of water after each dipping. Before the start of the alternate dipping the glass and quartz substrate were cleaned in Piranha solution and the surface phosphorylation was done by being kept in an acetonitrile solution of both 10 mM  $\text{POCl}_3$  and 2,6-lutidine for 2 h.<sup>10</sup> For ITO/glass the phosphorylation could not be done because ITO was removed in the  $\text{POCl}_3$  solution. Hence, ITO/glass was first cleaned in KOH/isopropanol solution and kept in 20 mM  $\text{ZrOCl}_2$  for 30 min and washed thoroughly with water to get Zr-rich surface.

## RESULTS AND DISCUSSION

The UV-Vis absorption spectra of EPNI and EPPI were first measured in aqueous solutions. EPNI was highly soluble in water regardless of solution pH but EPPI was soluble at pH higher than 4. Fig. 1 shows the absorption spectra of EPNI and EPPI at various pHs, compared with the spectra of their precursors, NTCD and PTCD that were hydrolyzed in basic solution and have the same main chromophores. EPNI showed the typical well-resolved bisimide spectrum that has the consecutively increasing peaks at 345, 362 and 383 nm.<sup>11</sup> It was very slowly hydrolyzed to amide at the pH higher than 10.<sup>12</sup> The precursor NTCD was not soluble in water before hydrolysis but it could be soluble in water after hydrolysis at pH higher than 10. It was known to be easily hydrolyzed at high pH to tetracarboxylate via the intermediate mono-anhydride.<sup>13</sup> Its absorption spectrum had an unresolved broad band at 308 nm as shown in Fig. 1(a). When EPNI was hydrolyzed at high pH, the spectrum was changed to similarly that of the hydrolyzed NTCD.

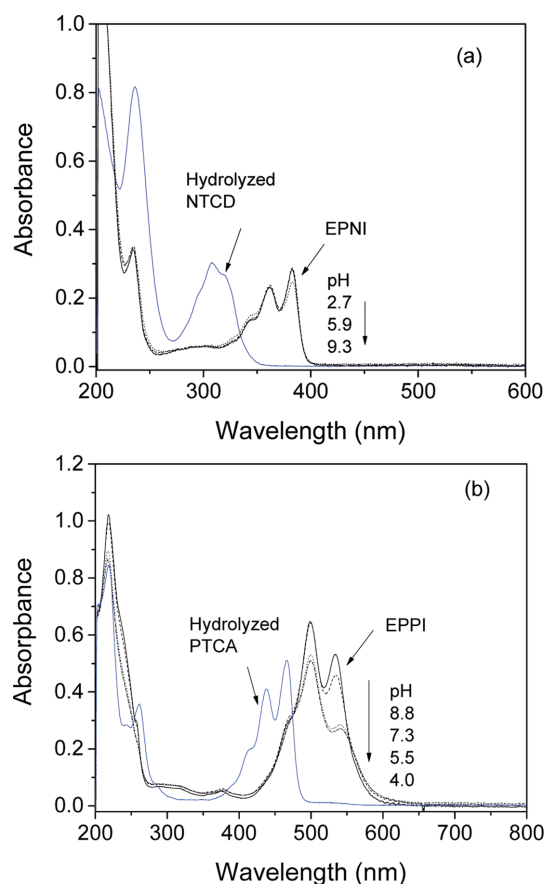


**Figure 1.** UV-Vis absorption spectra of (a) EPNI and hydrolyzed NTCD and (b) EPPI and hydrolyzed PTCD at various pHs (EPNI:  $4.4 \times 10^{-5}$  M, NTCD:  $2.8 \times 10^{-5}$  M, pH 9.1; EPPI:  $1.7 \times 10^{-5}$  M, PTCD:  $1.2 \times 10^{-5}$  M, pH 10).

The absorption spectrum of EPPI was strongly dependent on the solution pH as shown in *Fig. 1(b)*. EPPI could not seem to be in a monomeric form differently from EPNI because of the stronger interaction of aromatic ring. In a monomeric form a typical spectrum of perylene bisimide also shows the consecutively increasing three peaks like the spectrum of EPNI.<sup>14</sup> Unlike EPNI, the spectrum of EPPI in aqueous solution of pH higher than 7 has a maximum peak at 499 nm with a second peak at 534 nm. As pH decreased, the second peak at 534 nm decreased and was shifted to red as shown in *Fig. 1(b)*. The spectrum at the lowest pH was similar to that of the dimeric form of the carboxylate-terminated perylene bisimide.<sup>15</sup> There must be the monomer-dimer equilibrium in aqueous solution of EPPI, which depends on pH and concentration as previously demonstrated for the carboxylate-terminated perylene bisimide. Therefore, the monomer and dimer or polymeric forms where the chromophores were stacked by aromatic ring interaction coexisted in the measured pH range. The increased

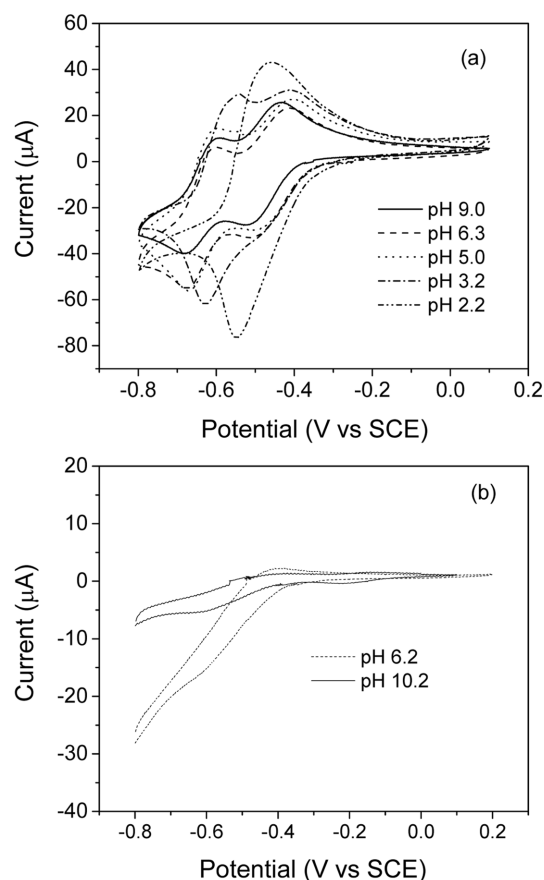


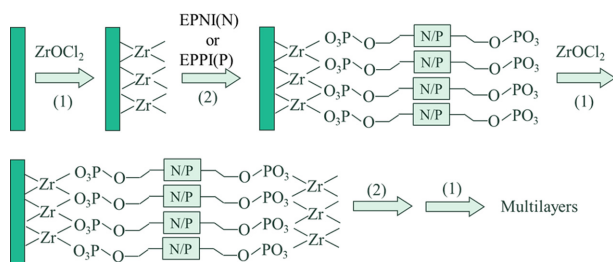
**Figure 2.** Cyclic voltammograms of (a) EPNI and (b) EPPI in 0.1 M KCl at various pHs (The scan rate: 50 mV/s, the concentrations of EPNI and EPPI were both 0.5 mM).

intensity of the second peak as pH increased indicates that the more monomeric form exists in higher pH.

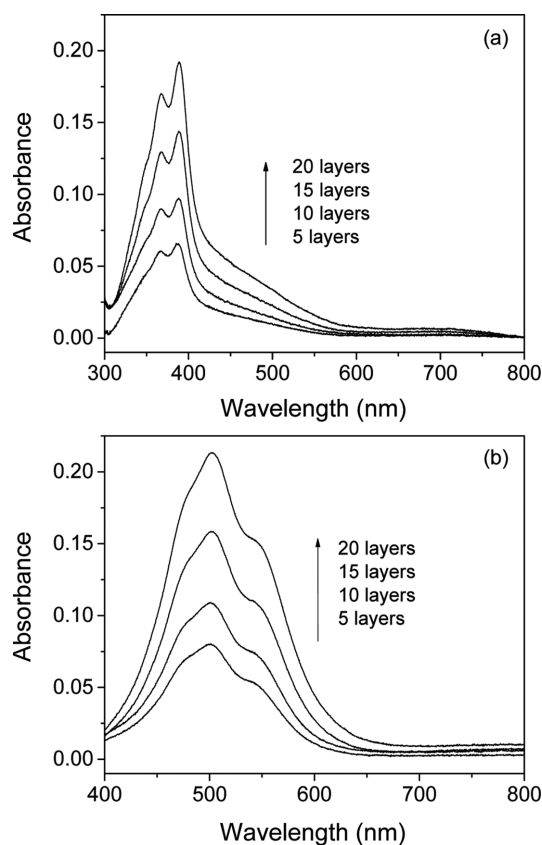
The redox properties of EPNI and EPPI in aqueous solution were examined by cyclic voltammetry. *Fig. 2(a)* shows the cyclic voltammogram of EPNI at various pHs. There were two distinctive quasi-reversible redox peaks that gave the half-wave potentials ( $E_{1/2}$ ) of  $-0.47$  and  $-0.64$  V vs SCE at pH higher than 5 corresponding to the formation of the radical-anion and dianion of the bisimide.<sup>16</sup> However, the second peak was incorporated to the first peak with the increased intensity as pH decreased and the almost single redox peak was observed with  $E_{1/2} = -0.50$  V at the pH below 2.5. This means that the first reduction did not depend on pH but the second did. This result might be explained by the fact that proton stabilized the reduced anionic radical formed by the first reduction and the second reduction potential was shifted to positive and the two potential became very close at the pH below 2.5. Differently from EPNI, EPPI did not show the reversible redox peaks in solution although perylene bisimide was also known to have typ-

ical two reversible reductions.<sup>17</sup> Only the weak reduction current was observed at the pH higher than 6 as shown in *Fig. 2(b)*. Since EPPI was precipitated in 0.1 M KCl solution even at pH 5 due to the high ionic strength of the electrolyte solution, the redox property of EPPI in solution was not observed at lower pH. As mentioned earlier, most of EPPI did not exist in the form of monomer in aqueous solution and it could be easily aggregated in the high concentration electrolyte solution. Therefore, the electron transfer between the dimeric or the aggregated EPPI in solution and the electrode might be difficult.

The multilayers of Zr-EPNI and Zr-EPPI were formed on the planar substrates of glass, quartz and ITO/glass by the alternate coordination of zirconium ion and the end group phosphate of EPNI and EPPI as shown in *Scheme 1*. The anchoring step to glass and quartz substrates was done by surface phosphorylation that were first time introduced by Katz et al.<sup>11</sup> but this procedure could not be applied to ITO substrate because ITO was stripped off in the phosphoryl chloride solution. So ITO/glass was treated with zirconyl chloride and both EPPI and EPNI were well adsorbed on Zr-rich surface. The multilayer growths were monitored by the absorption spectra as shown in *Fig. 3*. The absorption spectrum of Zr-EPNI multilayer was very similar to that of EPNI solution although the peaks were less resolved and there were small broad shoulder band in visible region. The maximum peak was slightly shifted to red as much as 6–7 nm. The absorbance increment was very systematic as the numbers of layer increased as previously demonstrated. The peak position was not also changed as the number of the layer increased, which means that there was no serious chromophore interaction between the layers (*inter* layer interaction). But the less resolved and the slight red-shifted spectrum, compared with one in solution, indicates that the chromophores in the same layer interacted each other (*intra* layer interaction) due to their close packing. The visible shoulder band that did not exist in solution might also indicate another kind of intralayer chromophore



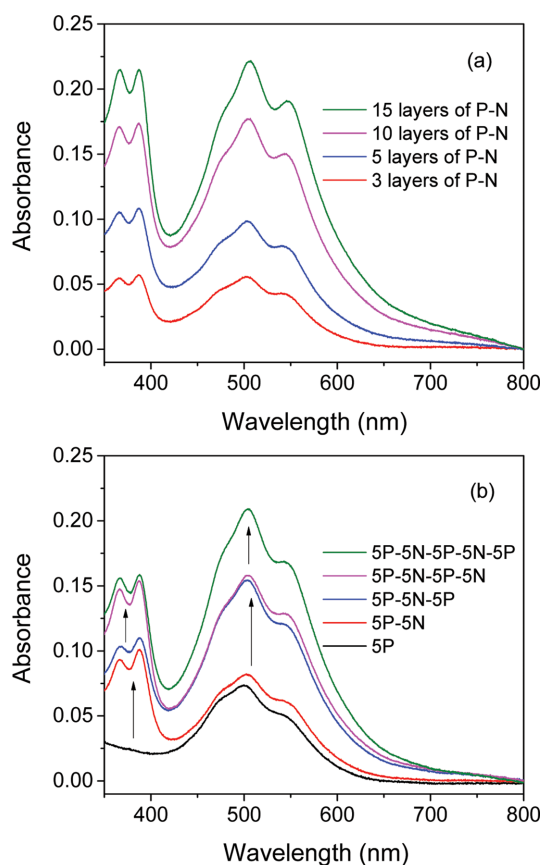
**Scheme 1.** Schematic drawing of the sequential adsorption method of Zr-EPNI or Zr-EPPI multilayers.



**Figure 3.** UV-Vis absorption spectra of the multilayers of (a) Zr-EPNI on quartz and (b) Zr-EPPI on glass substrate.

interaction. Zr-EPPI multilayer also showed the slightly different spectrum from that of the solution. The spectrum was more similar to that measured at the lowest pH but less resolved since the intralayer chromophore interaction could be stronger than that of the dimer or the polymeric forms in solution. The layer-by-layer growing was also quite systematic as EPNI did. The unchanged peak position according to the layer growth also tells that there was no interlayer chromophore interaction, either.

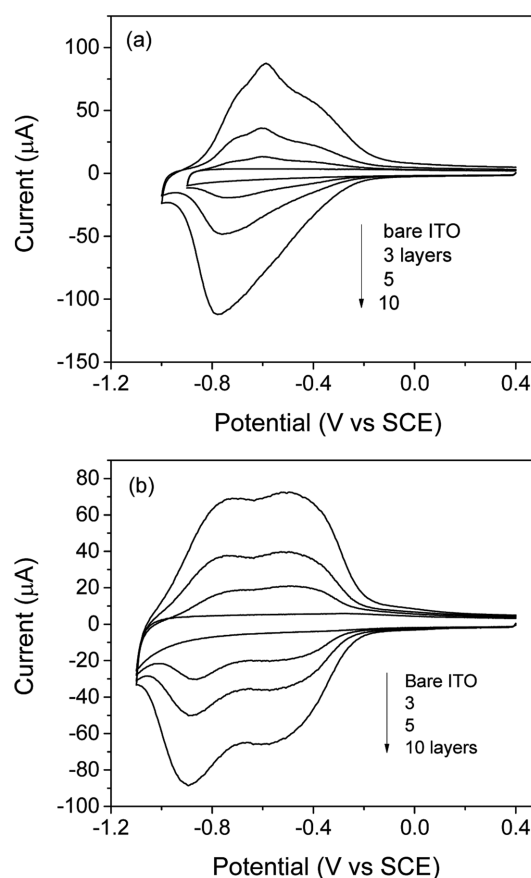
The mixed multilayers of Zr-EPNI and Zr-EPPI could be also formed by the adsorptions of alternate EPNI and EPPI. *Fig. 4(a)* shows the absorption spectra of one-by-one multilayers of Zr-EPNI and Zr-EPPI. Both the typical absorption peaks of EPNI and EPPI were shown together in the spectrum of the mixed multilayers. The repeating of the alternate layer adsorptions also gave very systematic growth of both the layers as monitored in the spectra. The multilayers of the alternate 5 Zr-EPNI and 5 Zr-EPPI layers were also prepared in order to confirm the independence of layer growing. As shown in *Fig. 4(b)*, the growing of the alternate 5 layers of Zr-EPPI and Zr-EPPI gave the



**Figure 4.** UV-Vis absorption spectra of the mixed multilayers of Zr-EPNI and Zr-EPPI on glass: (a) one-by-one layers of Zr-EPNI and Zr-EPPI, (b) five-by-five layers of Zr-EPNI and Zr-EPPI (P and N in the figures indicate Zr-EPPI and Zr-EPNI, respectively).

stepwise increases of the absorption peaks corresponding to EPPI and EPNI. There was also no peak interference between EPPI and EPNI. This means that no intrusion occurred between EPNI and EPPI layers. Therefore, the EPPI and EPNI layers could be grown independently on the top of each layer.

The redox properties of Zr-EPNI and Zr-EPPI multilayers on ITO electrode were investigated by the cyclic voltammetry. Fig. 5 shows the cyclic voltammograms of Zr-EPNI and Zr-EPPI multilayers on ITO electrode in 0.1 M KCl solution. Zr-EPNI multilayer showed almost single quasi reversible peak with  $E_{1/2} = -0.68$  V vs SCE although there were small shoulder oxidation peaks. The two step reductions of the bisimide that were shown in solution were not separated and the half-wave potential was close to the second redox potential of EPNI in neutral solution. On the contrary to Zr-EPNI, Zr-EPPI multilayer showed the two separate redox peaks with  $E_{1/2} = -0.54$  and  $-0.81$  V vs SCE. This is a somehow interesting result since only

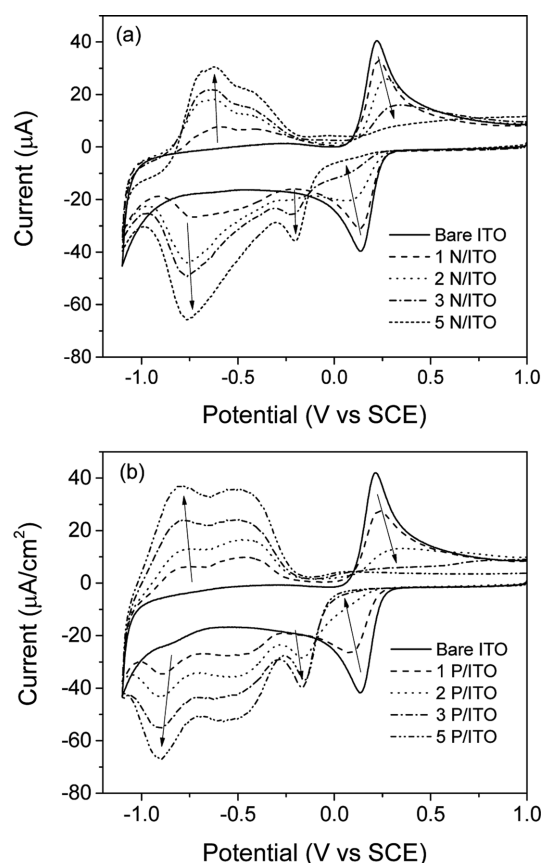


**Figure 5.** Cyclic voltammograms of the multilayers of (a) Zr-EPNI and (b) Zr-EPPI on ITO electrode in 0.1 M KCl electrolyte solution (The scan rate: 100 mV/s).

the irreversible weak peak was observed in the solution of EPPI. The electron transfer to the multilayer on the electrode surface seemed to be much easier than to the solution. The redox charges that were integrated from their voltammograms increased linearly as the number of layers increased. The surface coverages could be also calculated from the charges and the scan rate. The total charges and moles of the molecules were calculated and summarized in Table 1. The average layer densities of the molecules were  $1.5 \times 10^{-10}$  and  $2.3 \times 10^{-10}$  mol/cm<sup>2</sup> for Zr-EPNI and Zr-EPPI, respectively. These values are about one fifth and fourth of the surface coverage of octadecylphosphonate monolayer on SiO<sub>2</sub>/Si<sup>18</sup> and closely packed aliphatic chain monolayers.<sup>19</sup> Considering the molecular sizes of EPNI and EPPI, these coverages are understandable but the lower value for Zr-EPNI than for Zr-EPPI cannot be explained by size because the cross-sectional lengths of both molecules are same. The higher coverage for Zr-EPPI might be explained from the fact that the stronger aromatic ring interaction of EPPI could make the layer denser.

**Table 1.** The calculated values of reduction charges and moles of the multilayers from their cyclic voltammograms

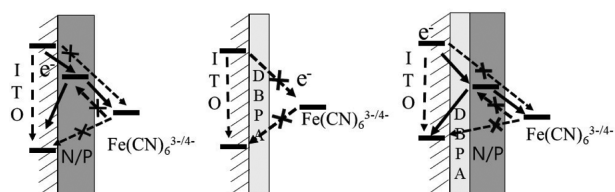
No. of Layers	Total charges of the multilayers ( $\times 10^{-5}$ C/cm $^2$ )		Total moles of the multilayers ( $\times 10^{-10}$ mol/cm $^2$ )	
	Zr-EPNI	Zr-EPPI	Zr-EPNI	Zr-EPPI
3	6.47	14.01	3.35	7.26
5	14.39	21.11	7.46	10.94
10	35.70	42.02	18.50	21.90
Average per layer	2.87	4.36	1.51	2.26

**Figure 6.** Cyclic voltammograms of bare ITO electrode and the multilayers of (a) Zr-EPNI (N) and (b) Zr-EPPI (P) on ITO electrode in aqueous 0.2 mM  $\text{K}_3\text{Fe}(\text{CN})_6$  and 0.1 M KCl solution. (The scan rate: 100 mV/s).

The electron transfers mediated by Zr-EPNI and Zr-EPPI multilayers were studied with a redox couple,  $\text{Fe}(\text{CN})_6^{3-}$  in solution. Fig. 6 shows the cyclic voltammograms of Zr-EPNI and Zr-EPPI multilayers on ITO electrode with 0.2 mM  $\text{K}_3\text{Fe}(\text{CN})_6$  in 0.1 M KCl solution. The reversible ferricyanide redox peaks were only shown with  $E_{1/2} = +0.18$  V vs SCE for bare ITO electrode. As both the numbers of Zr-EPNI and EPPI layers increased, the ferricyanide redox peaks decreased and the broad redox peaks of the multilayers appeared and increased. Simultaneously a new reduction peak appeared as a shoulder peak and increased near at

$-0.16$  and  $-0.20$  V vs SCE for Zr-EPNI and Zr-EPPI layers, respectively. The new shoulder peak did not keep increasing consecutively and the increase stopped after 5–6 layers of both the multilayers while the broad redox peaks of the multilayers kept increasing. The layers of both Zr-EPNI and Zr-EPPI seemed to block the direct electron transfer between ferricyanide in solution and ITO. One layer of each was not enough to block the electron transfer completely and the complete blockings were done by 5 layers of Zr-EPNI and 3 layers of Zr-EPPI. This is reasonable because Zr-EPPI layer was denser than Zr-EPNI as shown in the preceding discussion. The new shoulder peak must be due to the mediated reduction of ferricyanide by the reduced multilayers because the peaks grew simultaneously with the attenuation of the direct reduction peak of ferricyanide and no oxidation peak was shown. It is obvious that the mediated reduction is possible, but the oxidation is not because the redox potential of the multilayers more negative than that of ferricyanide as depicted in Scheme 2. The mediated reduction of ferricyanide occurred at the slightly more negative potential for Zr-EPNI than for Zr-EPPI because the substantial reduction of Zr-EPNI started at more negative potential. Therefore, the multilayers on the electrode could mediate the electron transfer from a redox couple in solution to ITO electrode at a shifted potential in one-way.

DBPA, which was composed of single alkyl chain with phosphonic acid at both ends, was the first molecule that was used to demonstrate a well-packed dense multilayer of zirconium bisphosphonate by the sequential adsorption method.<sup>5</sup> Its monolayer (Zr-DBP) on Au electrode that was anchored by 4-mercaptobutylphosphonic acid (MBPA)

**Scheme 2.** Schematic drawing of the electron transfer mediation by the layers of Zr-DBP and Zr-EPNI (N) or Zr-EPPI (P) into ferricyanide in solution from ITO electrode.

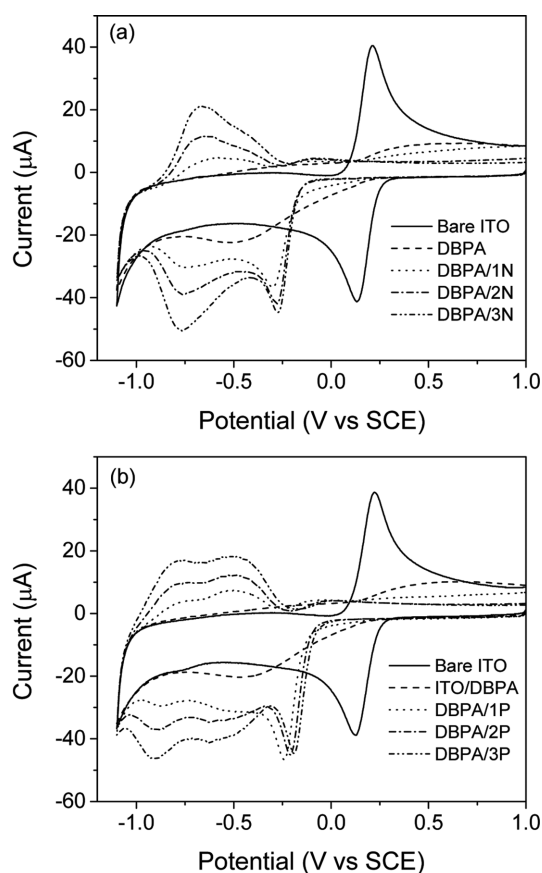


**Figure 7.** Cyclic voltammograms of bare ITO, Zr-DBP monolayer on ITO electrode and 1-3 layers of (a) Zr-EPNI (N) and (b) Zr-EPPI (P) on the top of Zr-DBP/ITO electrode in aqueous 0.2 mM  $\text{K}_3\text{Fe}(\text{CN})_6$  and 0.1 M KCl solution (The scan rate: 100 mV/s).

substantially blocked the electron transfer between ferricyanide in solution and the electrode.<sup>9</sup> DBPA was also well adsorbed directly on the surface of ITO treated with zirconyl chloride like EPNI and EPPI. We have prepared the multilayers of EPNI and EPPI on the top of Zr-DBP monolayer and checked the electron transfer between ferricyanide in solution and the modified electrode. When only the monolayer of Zr-DBP was covered on ITO, the redox peaks of ferricyanide nearly disappeared as shown in Fig. 7. However, when Zr-EPNI or Zr-EPPI layer was accumulated on the top of Zr-DBP monolayer, the mediated reduction peak immediately appeared with the broad redox peaks of the multilayers themselves and the mediated peak did not depend on the growth of the layers. This is somehow interesting because Zr-DBP monolayer blocked the electron transfer to the solution but did not block the transfer to Zr-EPNI or Zr-EPPI layer on itself. When ferrocene-linked benzylphosphonate was attached to Au electrode anchored by MBPA, very fast and reversible electron transfer occurred

through the spacer layer even though the distance between the electrode and ferrocene moiety was longer than  $\text{\AA}$ .<sup>20</sup> Since the thickness of Zr-DBP monolayer was estimated as about 17  $\text{\AA}$  in the previous study,<sup>5</sup> the electron transfer between ITO electrode and Zr-EPNI or Zr-EPPI layer through the spacer, Zr-DBP layer could be considered enough to be possible. Thus, the monolayer of Zr-EPNI and Zr-EPPI was not compact enough to block the direct redox reaction of ferricyanide in solution at the surface of ITO electrode. However, if even a monolayer of Zr-EPNI or Zr-EPPI has a sublayer of Zr-DBP on ITO surface, the direct redox reaction could be completely blocked and only the mediated reduction could occur. Thus, the electrochemically inactive sublayer could help the rectified electron transfer mediated by the electrochemically active layers. The enhanced rectification might be attributed to the fact that the insulating layer could provide the optimum energy barrier for the mediated electron transfer by blocking the direct electron transfer similarly like blocking layer in some dye sensitized solar cells.<sup>21</sup> The electron transfer routes between these modified electrodes and a redox couple in solution were depicted on Scheme 2.

## CONCLUSION

EPNI and EPPI that are naphthalene and perylene bisimide derivatives, respectively terminated with dihydrogen phosphate at both ends and their zirconium bisphosphate multilayers (Zr-EPNI and Zr-EPPI) were investigated. The electrochemical properties of EPNI and EPPI were quite different in aqueous solutions even though both naphthalene and perylene bisimides were known to have typical two reversible reductions. While EPNI showed two reversible reductions at high pH (that was reduced to one reduction at low pH), EPPI showed only an irreversible reduction at soluble pH. This result seemed to be due to the facts that EPNI was in monomeric form in aqueous solution, but EPPI was in dimeric or polymeric forms where perylene chromophores were stacked by stronger aromatic  $\pi$ -interaction than naphthalene. However, Both the Zr-EPNI and Zr-EPPI multilayers on ITO electrode showed reversible redox peaks even though Zr-EPNI have single broad peak and Zr-EPPI have two separated reversible peaks. The estimated layer densities of Zr-EPNI and Zr-EPPI were  $1.5 \times 10^{-10}$  and  $2.3 \times 10^{-10}$  mol/cm<sup>2</sup>, respectively. Zr-EPPI was denser than Zr-EPNI. Both the monolayers of Zr-EPNI and Zr-EPPI were not compact enough to block completely the electron transfer between ITO electrode and a redox couple,  $\text{Fe}(\text{CN})_6^{3-/4-}$  in solution while Zr-DBP monolayer that con-

sisted of a simple alkyl chain could block it much better. However, 3–5 layers of Zr-EPNI and Zr-EPPI were enough for blocking the direct electron transfer and both the multilayers could mediate the reduction of the ferricyanide in solution at a shifted potential but not for the oxidation. When a monolayer of Zr-DBP was used as a sublayer of Zr-EPNI and Zr-EPPI layer, the mediated electron transfer became prominent by even the monolayers as well as the direct electron transfer was completely blocked. Therefore, the combination of Zr-EPPI/EPNI and Zr-DBP layers can provide a good electrochemical rectification tool.

**Acknowledgments.** This work was supported by the research fund of Pukyong National University (Year 2017–2018).

## REFERENCES

1. “Bisimide” was used as a synonym of bis(dicarboximide). “Diimide” was more commonly used in many literatures instead of bisimide despite it also denotes diazene, i.e. “HN=NH”.
2. (a) Bhosale, S. V.; Jani, C. H.; Langford, S. J. *Chem. Soc. Rev.* **2008**, *37*, 331. (b) Kobaisi, M. A.; Bhosale, S. V.; Latham, K.; Raynor, A. M. *Chem. Rev.* **2016**, *116*, 11685.
3. (a) Huang, C.; Barlow, S.; Marder, S. J. *Org. Chem.* **2011**, *76*, 2386. (b) Kozma, E.; Catellani, M. *Dyes Pigments* **2013**, *98*, 160. (c) Würthner, F.; Saha-Möller, C. R.; Fimmel, B.; Ogi, S.; Leowanawat, P. *Chem. Rev.* **2016**, *116*, 962.
4. (a) Thompson, M. E. *Chem. Mater.* **1994**, *6*, 1168. (b) Katz, H. E.; Schilling, M. L.; Ungasche, S.; Putvinski, T. M.; Chidsey, C. E. Chapt. 3 in “*Supramolecular Architecture: Synthetic Control in Thin Films and Solids*” ACS Symp. Series 499, 1992, ed. Bein, T.
5. Lee, H.; Kepley, L. J.; Hong, H.-G.; Mallouk, T. E. *J. Am. Chem. Soc.* **1988**, *110*, 618.
6. (a) Katz, H. E.; Schilling, M. L.; Chidsey, C. E. D. Putvinski, T. M.; Hutton, R. S. *Chem. Mater.* **1991**, *3*, 699. (b) Vermeulen, L. A.; Thompson, M. E. *Nature*, **1992**, *358*, 656. (c) Katz, H. E.; Wilson, W. L.; Scheller, G. *J. Am. Chem. Soc.* **1994**, *116*, 6636. (d) Neff, G. A.; Helfrich, M. R.; Clifton, M. C.; Page, C. J. *Chem. Mater.* **2000**, *12*, 2363. (e) Masari, A. M.; Gurney, R. W.; Wightman, M. D.; Huang, K. C.-H.; Nguyen, S. T.; Hupp, J. T. *Polyhedron*, **2003**, *22*, 3065.
7. (a) Chae, H. J.; Kim, Y. I.; Kim, E.-R.; Lee, H. *Bull. Korean Chem. Soc.* **1998**, *19*, 27. (b) Lee, M. S.; Shim, H. K.; Kim, Y. I. *Mol. Cryst. Liq. Cryst.* **1998**, *316*, 401. (c) Chae, H. J.; Kim, Y. I.; Kim, E.-R.; Lee, H. *Mol. Cryst. Liq. Cryst.* **1998**, *316*, 179. (d) Cho, K. J.; Shim, H. K.; Kim, Y. I. *Syn. Metal.* **2001**, *117*, 153.
8. (a) Rodrigues, M. A.; Petri, D. F. S.; Politi, M. J.; Brochsztain, S. *Thin Solid Films* **2000**, *371*, 109. (b) Marcon, R. O.; K. M.; Brochsztain, S. *Thin Solid Films* **2005**, *492*, 30. (c) Marcon, R. O.; Santos, J. G.; Figueiredo, K. M.; Brochsztain, S. *Langmuir*, **2006**, *22*, 1680.
9. Lee, H.; Kepley, L. J.; Hong, H.-G.; Akhter, S.; Mallouk, T. E. *J. Phys. Chem.* **1988**, *92*, 2597.
10. Putvinski, T. M.; Schilling, M. L.; Katz, H. E.; Chidsey, C. E. D.; Muijsce, A. M.; Emerson, A. B. *Langmuir* **1990**, *6*, 1567.
11. Alp, S.; Erten, S.; Karapire, C.; Köz, B.; Doroshenko, A. O.; İçli, S. *J. Photochem. Photobiol. A: Chem.* **2000**, *135*, 103.
12. Kim, M. B. “*The hydrolysis of naphthalene diimides*” MS Thesis, Georgia State University, 2007.
13. Barros, T. C.; Cuccovia, I. M.; Farah, J. P. S.; Masini, J. C.; Chaimovich, H.; Politi, M. *J. Org. Biomol. Chem.* **2006**, *4*, 71.
14. Icli, S.; Demic, S.; Dindar, B.; Doroshenko, A. O.; Timur, C. *J. Photochem. Photobiol. A: Chem.* **2000**, *136*, 15.
15. Ford, W. *J. Photochem.* **1987**, *37*, 189.
16. Viehbeck, A.; Goldberg, M. J.; Kovac, C. A. *J. Electrochem. Soc.* **1990**, *137*, 1460.
17. (a) Ford, W. E.; Hiratsuka, H.; Kamat, P. V. *J. Phys. Chem.* **1989**, *93*, 6692. (b) Lee, S. K.; Zu, Y.; Herrmann, A.; Geerts, Y.; Mullen, K.; Bard, A. J. *J. Am. Chem. Soc.* **1999**, *121*, 3513.
18. Hanson, E. L.; Schwartz, J.; Nickel, B.; Koch, N.; Danisman, M. F. *J. Am. Chem. Soc.* **2003**, *125*, 16074.
19. Kitaigorodskii, A. I. *Organic Chemical Crystallography*; Consultants Bureau: New York, 1961.
20. Hong, H.-G.; Mallouk, T. E. *Langmuir*, **1991**, *7*, 2362.
21. Selopal, G. S.; Memarian, N.; Milan, R.; Concina, I.; Sberveglieri, G.; Volmiero, A. *ACS App. Mater. Interfaces* **2014**, *6*, 11236.